

Study of Asparagine 353 in Aminopeptidase A: Characterization of a Novel Motif (GXMEN) Implicated in Exopeptidase Specificity of Monozinc Aminopeptidases

Xavier Iturriz, Raphaël Rozenfeld, Annie Michaud, Pierre Corvol, and Catherine Llorens-Cortes*

INSERM Unité 36 – Collège de France, 11 place Marcelin Berthelot, 75005 Paris, France

Received July 9, 2001; Revised Manuscript Received September 17, 2001

ABSTRACT: Aminopeptidase A (EC 3.4.11.7, APA) is a 160 kDa membrane-bound zinc enzyme that contains the HEXXH consensus sequence found in members of the zinc metalloprotease family, the zincins. In addition, the monozinc aminopeptidases are characterized by another conserved motif, GXMEN, the glutamate residue of which has been shown to be implicated in the exopeptidase specificity of aminopeptidase A [Vazeux G. (1998) *Biochem. J.* 334, 407–413]. In carboxypeptidase A (EC 3.4.17.1, CPA), the exopeptidase specificity is conferred by an arginine residue (Arg-145) and an asparagine residue (Asn-144). Thus, we hypothesized that Asn-353 of the GXMEN motif in APA plays a similar role to Asn-144 in CPA and contributes to the exopeptidase specificity of APA. We investigated the functional role of Asn-353 in APA by substituting this residue with a glutamine (Gln-353), an alanine (Ala-353) or an aspartate (Asp-353) residue by site-directed mutagenesis. Expression of wild-type and mutated APAs revealed that Gln-353 and Ala-353 are similarly routed and glycosylated to the wild-type APA, whereas Asp-353 is trapped intracellularly and partially glycosylated. Kinetic studies, using α -L-glutamyl- β -naphthylamide (GluNA) as a substrate showed that the K_m values of the mutants Gln-353 and Ala-353 were increased 11- and 8-fold, respectively, whereas the k_{cat} values were decreased (2-fold) resulting in a 24- and 14-fold reduction in cleavage efficiency. When α -L-aspartyl- β -naphthylamide or angiotensin II were used as substrates, the mutations had a greater effect on k_{cat} , leading to a similar decrease in cleavage efficiencies as that observed with GluNA. We then measured the inhibitory potencies of several classes of inhibitors, glutamate thiol, glutamine thiol and two isomers (L- or D-) of glutamate phosphonate to explore the functional role of Asn-353. The data indicate that Asn-353 is critical for the integrity and catalytic activity of APA. This residue is involved in substrate binding via interactions with the free N-terminal part and with the P1 carboxylate side chain of the substrate. In conclusion, Asn-353 of the GXMEN motif, together with Glu-352, contributes to the exopeptidase specificity of APA and plays an equivalent role to Asn-144 in CPA.

Aminopeptidase A (EC 3.4.11.7, APA)¹ is a 160 kDa homodimeric type II membrane-bound zinc metalloprotease that specifically cleaves the N-terminal glutamyl or aspartyl residue from peptide substrates such as angiotensin II (Ang II) and cholecystokinin-8 in vitro (1, 2). APA is expressed in many tissues, particularly the brush border of the intestinal and renal epithelial cells and in the vascular endothelium (3). APA is also present in brain nuclei with other components of the brain renin-angiotensin system (4). Studies with specific and selective APA inhibitors (5) have shown that in the brain APA is involved in the conversion of Ang II to angiotensin III (Ang III) (6) and that brain Ang III exerts a tonic stimulatory action on the central control of blood

pressure (7). This suggests that brain APA constitutes a putative central therapeutic target for the treatment of hypertension (reviewed in ref 8). The determination of the complete amino acid sequence of APA in mouse (9), man (10, 11), rat (12), and pig (13) revealed an HEXXH consensus sequence, which is found in the zinc metalloprotease family, the zincins (14, 15). The amino acid sequence of APA is 22–35% homologous to those of other monozinc aminopeptidases such as rat aminopeptidase N (EC 3.4.11.2, APN) (16, 17), rat aminopeptidase B (EC 3.4.11.6, APB) (18, 19), thyrotropin-releasing hormone-degrading enzyme (EC 3.4.19.6, TRH degrading enzyme) (20), human leukotriene A4 hydrolase (EC 3.3.2.6, LTA4 hydrolase) (21) and human placental leucine aminopeptidase/oxytocinase also called insulin-responsive aminopeptidase (EC 3.4.11.3, P-LAP, IRAP) (22), with the greatest sequence conservation in the region flanking the zinc-binding motif. In the absence of structural data on monozinc aminopeptidases, site-directed mutagenesis was used to elucidate the organization of the mouse APA active site on the basis of sequence alignment of APA with monozinc aminopeptidases. First, Wang and Cooper (23) identified the histidine 389 of the APA HEXXH (385–389) motif as one of the three zinc ligands. Subse-

* To whom correspondence should be addressed. Phone: (331) 44.27.16.63. Fax: (331) 44.27.16.91. E-mail: c.llorens-cortes@college-de-france.fr.

¹ Abbreviations: APA, aminopeptidase A; APN, aminopeptidase N; APB, aminopeptidase B; TRH, thyrotropin-releasing hormone; LTA4, leukotriene A4; P-LAP, placental leucine aminopeptidase; TLN, thermolysin; CPA, carboxypeptidase A; bLAP, bovine lens leucine aminopeptidase; NEP 24.11, neutral endopeptidase; WT, wild-type; Ang II, angiotensin II; GluNA, α -L-glutamyl- β -naphthylamide; AspNA α -L-aspartyl- β -naphthylamide; GluPO₃H₂, glutamate phosphonic acid; GluSH, glutamate thiol; GlnSH, glutamine thiol.

	353	386
APA mouse	: KIAIPDFGT GAME N WGLVTYRETNLLYDPLLSASSNQQRVASVVA HEL VHQWFGNTVTDWWDLDWLNE	
APA human	: KIAIPDFGT GAME N WGLITYRETNLLYDPKESASSNQQRVATVVA HEL VHQWFGNIVTMDWWDLDWLNE	
APN human	: QIGLPDFNA GAME N WGLVTYRENSLFDPLSSSSSNKERVVTVIA HEL AHQWFGNLVTIEWWDLWLNE	
APN rat	: QIALPDFNA GAME N WGLVTYRESALVFDPSSSISNKERVVTVIA HEL AHQWFGNLVTVDWWDLDWLNE	
APN mouse	: QIALPDFNA GAME N WGLVTYRESSLVFDSQSSISNKERVVTVIA HEL AHQWFGNLVTVAWWDLWLNE	
IRAP rat	: LVAIPDFEA GAME N WGLLTFREETLLYDNATSSVADRKLVTKI IA HEL AHQWFGNLVTVQWWDLDWLNE	
PSA mouse	: -IAIADFAA GAME N WGLVTYRETAALLIDPKNSCSSSRQWVALVVG HEL AHQWFGNLVTMEWWTHLWLNE	
APEII yeast	: NVAVHEFS GAME N WGLVTYRVVLLDKDNSTLDRIQRVAEVVQ HEL AHQWFGNLVTVMDWWEGLWLNE	
LTA4H rat	: ---PSFPY GME N PCLTFVTPTLLAGDKSLS-----NVIA HEI SHSWTGNLVTNKTWDHFWLNE	
LTA4H mouse	: ---PSFPY GME N PCLTFVTPTLLAGDKSLS-----NVIA HEI SHSWTGNLVTNKTWDHFWLNE	
LTA4H human	: ---PSFPY GME N PCLTFVTPTLLAGDKSLS-----NVIA HEI SHSWTGNLVTNKTWDHFWLNE	
APB rat	: ---PSFPF GME N PCLTFVTPTLLAGDR-----SLADV II HEI SHSWFGNLVTNANWGEFWLNE	
	69	144
CBPA human	: IDTGI HSRE WVTQASGVWFAKKITQDY...34aa...MWRKTRSHTAGSLCIGVDF NRN WDAGFGLS	
CBPB human	: IDCIG HARE WIGPAFCQWVKEALLTY...34aa...FWRKTRSRNSRFRRCRGVDA NRN WKVKGCGK	
CBPD human	: YIGNM HGNE VVGRELLNLIEYLCKNF...29aa...QEGDSISVIGRNNSNFDL NRN FPDQFVQI	
CBPE human	: YIGNM HGNE AVGRELLIFLAQYLCNEY...33aa...PGELKDWVFGRSNAQGIDL NRN FPDLDRIV	

FIGURE 1: (A) Alignment of the mouse APA amino acid sequence with the sequences of other monozinc aminopeptidases. The consensus zinc-binding motif, HEXXH, is indicated in italics, the conserved residues are indicated in bold. The conserved motif, GXMEN, is in bold. In this motif, asparagine 353 of APA and its homologous residues in other sequences are indicated in large, bold letters. Alignment of the amino acid sequences of mouse and human APA (APA, EC 3.4.11.7); human, rat and mouse aminopeptidase N (APN, EC 3.4.11.2); rat insulin-regulated membrane aminopeptidase (IRAP); mouse puromycin-sensitive aminopeptidase (PSA, EC 3.4.11.14); yeast aminopeptidase II (APEII); rat, mouse and human LTA4 hydrolase (LTA4H, EC 3.3.2.6); rat APB (APB, EC 3.4.11.6). (B) Amino acid sequence alignment of different zinc carboxypeptidases. The consensus zinc binding sequence HXXE is indicated in italics, the conserved residues are indicated in bold. The conserved motif NRN is in bold. In this motif, asparagine 144 of carboxypeptidase A and its homologous residues in other carboxypeptidases are indicated in large, bold letters. Alignment of human carboxypeptidase A (CBPA, EC 3.4.17.1), human carboxypeptidase B (CBPB, EC 3.4.17.2), human metallocarboxypeptidase D (domain 2), (CBPD, EC 3.4.17.22), human carboxypeptidase E (CBPE, EC 3.4.17.10).

quently, we showed that Glu-408 in the APA WLNEG (405–409) motif, which is conserved among the different monozinc aminopeptidases, constitutes the third zinc ligand and that Glu-386 located in the HEXXH zinc-binding motif plays a critical role in catalysis and is the catalytic effector in APA (24). Interestingly, alignment of the sequence of APA with the sequences of several monozinc aminopeptidases in the region surrounding the zinc binding motif revealed a conserved tyrosine residue (Tyr-471 in APA). Site-directed mutagenesis studies on Tyr-471 showed that this residue is essential for the catalytic activity of APA. The role of Tyr-471 in catalysis is to stabilize the transition state complex through interaction of its hydroxyl group with the oxyanion of the tetrahedral intermediate via a hydrogen bond (25). Moreover, His-450 in APA is involved in substrate binding via an interaction with the P1 carboxylate side chain of the substrate and may contribute with Ca^{2+} to the substrate specificity of this enzyme for N-terminal acidic amino acid residues (26). Sequence alignment also revealed the presence of the conserved motif, GXMEN (348–353 in APA), in which Glu-352 plays a crucial role in the catalytic process of APA and contributes to the exopeptidase activity of this enzyme by interacting with the N-terminal part of the substrate (27). These data are consistent with those recently obtained with the crystallographic structure of the bifunctional enzyme (epoxyde hydrolase/aminopeptidase) LTA4 hydrolase (28). Comparison with other zinc-metalloproteases shows that some residues in APA may have similar functions to those of other exopeptidases such as carbox-

ypeptidase A (EC 3.4.17.1, CPA), or two-zinc containing aminopeptidase such as bovine lens leucine aminopeptidase (EC 3.4.11.1, bLAP) despite the very low sequence identity between these enzymes. For example, the exopeptidase specificity of monozinc aminopeptidases is attributed to an acidic residue (glutamate) that binds the free amino terminal group of the substrate, and the exopeptidase specificity of zinc metallocarboxypeptidases is due to a basic residue (arginine) that binds the free carboxylate terminal group of the substrate (27–30). However, the exopeptidase specificity of CPA is conferred by both arginine 145 (Arg-145) and asparagine 144 (Asn-144), which are found in the NRN-(144–146) motif that is conserved among zinc metallocarboxypeptidases (Figure 1B), and both of which contribute to the binding of the free carboxylate terminal group of the substrate (31). Sequence alignment of APA with several monozinc aminopeptidases (Figure 1A) revealed the presence of a strictly conserved asparagine residue (Asn-353 in APA) in the conserved GXMEN motif located 31 residues from the zinc-binding motif HEXXH. We therefore hypothesize that the GXMEN motif of APA corresponds to the NRN motif of CPA. Asn-353 in the GXMEN motif in APA may play a similar role to Asn-144 in CPA and thus could contribute with Glu-352 to the exopeptidase specificity of APA. To verify this hypothesis, we used site-directed mutagenesis to investigate the functional role of this residue by replacing Asn-353 with a glutamine, an alanine and an aspartate. We subsequently biochemically and kinetically

characterized purified recombinant wild-type and mutated enzymes to determine the role of this residue.

EXPERIMENTAL PROCEDURES

Materials. Restriction endonucleases and DNA-modifying enzymes were obtained from New England Biolabs (Hitchin, England) and were used according to the manufacturer's instructions. DNA Taq polymerase isolated from *Pyrococcus furiosus* (Pfu) was purchased from Stratagene (La Jolla, CA). The liposomal transfection reagent, Dosper, was purchased from Roche (Mannheim, Germany). The pcDNA 3.1 His vector and the anti-Xpress antibody were purchased from Invitrogen (Groningen, The Netherlands). Immobilized cobalt affinity columns (Talon) were obtained from Clontech (Heidelberg, Germany). The synthetic substrates, α -L-glutamyl- β -naphthylamide (GluNA) and α -L-aspartyl- β -naphthylamide (AspNA) and the natural substrate, angiotensin II were purchased from Bachem (Bubendorf, Switzerland).

Methods. (i) *Cloning and Site-Directed Mutagenesis.* The mouse cDNA encoding APA (23) cloned in the expression vector pcDNA 3.1 His was mutated by site-directed mutagenesis performed by polymerase chain reaction (PCR) as previously described (32). Two overlapping regions of the cDNA were amplified separately using two flanking oligonucleotides: A (5'-CAGAAGGAGACAGCAGAGTATG-3', position 919–940 bp) as a sense primer and B (5'-TGCCTCTTGACAGTGAATCCCA-3', position 1534–1554 bp) as a reverse primer and two overlapping oligonucleotides (C1D1 for Gln-353, C2D2 for Ala-353 and C3D3 for Asp-353) at position 1043–1066 bp that contained the mutations C1, 5'-CCGGCGCCATGGAACAATGGGGAC-3'; C2, 5'-CCGGCGCCATGGAAGCTTGGGGAC-3'; C3, 5'-CCGGCGCCATGGAAGAATGGGGAC-3'; D1, 5'-GTCCCCAT-TGTTCCATGGCGCCGG-3'; D2, 5'-GTCCCCAAGCTTCC-ATGGCGCCGG-3'; D3, 5'-GTCCCCATTTCTTCATG-GCGCCGG-3'. The underlined bases encode the new amino acid residue replacing asparagine at position 353. Nucleotide numbering refers to the mouse APA sequence (9) deposited in the GenBank database (accession number M29961).

The products of the two first amplifications (A–D and B–C) were used for a further PCR with the two flanking oligonucleotides A and B. For all PCR, Pfu (1 unit) was used (25 cycles: 94 °C, 30 s; 54 °C, 45 s; 72 °C, 2 min). A final 635 bp PCR product containing the unique restriction sites *SgrAI* and *EcoRV* was obtained. After digestion with *SgrAI* and *EcoRV* the fragment was purified from the agarose gel and the 360 bp *SgrAI*–*EcoRV* fragment containing the mutation was used to replace the corresponding nonmutated region (*SgrAI*–*EcoRV*) of the full-length APA cDNA. The presence of the mutation and the absence of nonspecific mutations was confirmed by automated sequencing using an Applied Biosystems 377 DNA Sequencer and dye deoxy-terminator chemistry.

(ii) *Cell Culture and Establishment of Pure CHO-K1 Cell Lines Expressing Wild-Type and Mutated His-APAs.* CHO-K1 cells were maintained in Ham's F12 medium supplemented with 7% fetal calf serum, 0.5 mM glutamine, 100 units/mL penicillin, and 100 μ g/mL streptomycin (all from Boehringer-Mannheim, Germany). To establish pure cell lines expressing the polyhistidine tagged wild-type and

mutated His-APA enzymes, a liposomal transfection reagent (Dosper) (6 μ g) was used to transfect CHO-K1 cells with 1 μ g of the corresponding plasmids. Transfected cells were grown in a humidified 5% CO₂/95% air atmosphere and were selected for resistance to 750 μ g/mL Geneticin G418 (Gibco-BRL, Cergy Pontoise, France). Individual resistant colonies, producing large amounts of APA were cloned by limiting dilution techniques.

(iii) *Immunofluorescence of Stable Transfected CHO Cells.* Stable transfected CHO cells were seeded at 10⁴ cells on 12 mm diameter coverslips and grown overnight in Ham's F12 medium in a humidified atmosphere of 5% CO₂/95% air. Ninety minutes before the immunofluorescence, cells were incubated with cycloheximide (70 μ M) in Ham's F12 medium. Then the cells were fixed and permeabilized for 5 min in 100% ice-cold methanol. The cells were rinsed three times in 0.1 M phosphate buffered saline, pH 7.4 (PBS), and saturated with 5% BSA for 30 min at room temperature (RT), before being incubated with 1:500 dilution of polyclonal rabbit anti-(rat APA) serum (33) in PBS, 2% BSA (100 μ L/coverslip) for 90 min at RT. The coverslips were washed three times with cold PBS and incubated with 1:500 dilution of polyclonal anti-rabbit antibody conjugated with cyanin 3 for 2 h at RT. After washing (four times) with PBS, the preparation was mounted with Mowiol (Sigma-Aldrich, Germany) for confocal microscopic examination.

Cells were examined with a Leica TCS SP II (Leica Microsystems, Heidelberg, Germany) confocal laser scanning microscope configured with a Leica DM IRBE inverted microscope equipped with an argon/krypton laser. Cyanin 3 (Cy3) fluorescence was detected with 100% excitation at 550 nm, using a RSP 500 dichroic mirror and the spectrophotometer set to acquire emission at 570 nm. Images of 1024 \times 1024 pixels of cells were obtained using a 63 \times 1.32 NA oil-immersion objective with zoom 2.

(iv) *Metabolic Labeling and Immunoprecipitation.* Stable transfected CHO cells (300 000 cells/well) were incubated for 30 min in methionine-cysteine serum free medium (Ham's 12) containing 100 μ Ci/mL of [³⁵S]methionine/cysteine (pulse). The cells were then incubated for different times (0, 1, and 2 h) in complete Ham's F12 medium (chase). After discarding the cell medium, cells were harvested and proteins were solubilized overnight at 4 °C with 600 μ L of 50 mM Tris-HCl buffer, pH 7.4, 150 mM NaCl, 10 mM EDTA, 1% (v/v) Triton X-100 and then centrifuged 20000g for 5 min at 4 °C. The solubilized fraction was immunoprecipitated with a polyclonal rabbit anti-(rat APA) serum (1 μ L) (33) and protein A-sepharose (Pharmacia-LKB Biotechnology) [50% (w/v) suspension in solubilization buffer] for 4 h at 37 °C. The immune complexes were collected by centrifugation and washed four times with solubilization buffer and once with 20 mM Tris-HCl buffer, pH 6.8. Proteins were eluted by boiling in 25 μ L of Laemmli buffer and resolved by 7.5% SDS–polyacrylamide gel electrophoresis (SDS–PAGE) as described by Laemmli (34). The dried gel was then exposed for autoradiography.

(v) *Production and Purification of Recombinant APAs.* Stable transfected CHO cells were harvested, and membrane preparation was performed as previously described (26). The wild-type and mutated recombinant His-APAs were purified with Talon technology as previously described (26). Protein concentrations were determined by the Bradford assay using

bovine serum albumin as the standard. We systematically verified that the protein concentration estimated by the Bradford assay for the different recombinant APAs reflects the true APA concentration. For this purpose, we estimated the concentration of APA by performing dot blots of purified recombinant APAs using anti-Xpress antibody (dilution 1:5000). Immunoreactive material was detected with an anti-mouse antibody coupled to horseradish peroxidase (HRP) (1:12000) and resolved by ECL western blotting reagents (Amersham, England). The chemiluminescence was measured by microdensitometric scanning of the dot-blot. Protein fractions were resolved by 7.5% SDS-PAGE. Proteins were stained with Coomassie Brilliant blue R-250 or transferred to a nitrocellulose membrane by liquid transfer in 25 mM Tris/glycine buffer, pH 8.3, containing 10% (v/v) methanol. His-tagged recombinant proteins were detected with the anti-Xpress antibody (dilution 1:5000). The immune complex was detected as described above.

(vi) *Enzyme Assay.* (a) *GluNA and AspNA Hydrolysis.* The activities of the wild-type and mutated His-APAs were determined in a microtiter plate, by monitoring the rate of hydrolysis of a synthetic substrate, α -L-glutamyl- β -naphthylamide (GluNA) or α -L-aspartyl- β -naphthylamide (AspNA), as previously described (35). Purified wild-type and mutated recombinant His-APAs were incubated at 37 °C in the presence of various concentrations of GluNA or AspNA with 4 mM CaCl_2 in a final volume of 100 μL of 50 mM Tris-HCl buffer, pH 7.4.

(b) *Angiotensin II Hydrolysis.* Purified wild-type and mutated recombinant His-APAs were incubated at 37 °C in the presence of various concentrations of angiotensin II with 0.5 mM CaCl_2 in a final volume of 250 μL of 50 mM Hepes buffer, pH 7.4, and the reaction was terminated by the addition of 50 μL of 12% H_3PO_4 . The activities of wild-type and mutated His-APAs were determined by monitoring the rate of conversion of angiotensin II to angiotensin III by high-performance liquid chromatography (HPLC) on a Waters apparatus directed by a millennium chromatography manager. The formation of angiotensin III was followed and quantified by isocratic reversed-phase HPLC on a Hypersil C18 ODS-3 μm at 45 °C in 15% (v/v) acetonitrile, and 86 mM triethylammonium phosphate, pH 3.0, at a flow rate of 1 mL/min. Retention times for angiotensin II and angiotensin III were 11 and 9 min, respectively, with a detection limit of 0.1 nmol at 200 nm.

The kinetic parameters (K_m and k_{cat}) were determined from Lineweaver-Burk plot with a final concentration of GluNA between 0.025 and 2 mM and a final AspNA and angiotensin II between 0.025 and 1 mM. The sensitivity of wild-type and mutated His-APAs to glutamate thiol (D-,L-) (GluSH) (36), glutamine thiol (D-,L-) (GlnSH) (35), glutamate phosphonic acid (L-) or (D-) (GluPO_3H_2) (37, 38) was determined by establishing dose-dependent inhibition curves at a final GluNA concentration of 0.5 mM and calculating K_i values with Graph Pad Prism 2 software. A concentration of 0.2 mM of GluNA was used for the determination of the K_i value of captopril (39). Statistical comparisons were performed with Student's unpaired t test. Differences were considered significant if p was less than 0.05.

RESULTS

Site-Directed Mutagenesis of His-APA cDNA. Sequence alignment of mouse APA with other monozinc aminopeptidases in the region flanking the zinc-binding motif revealed a strictly conserved GXMEN motif upstream of the HEXXH motif (Figure 1A). Site-directed mutagenesis studies of Glu-352 in APA showed that this residue is involved in the catalytic process of APA and contributes to the exopeptidase activity of this enzyme by interacting with the free N-terminal part of substrates (27). Luciani et al. reported similar findings on an equivalent residue in APN (Glu-350) (30). To further characterize the conserved GXMEN motif of APA, we studied the functional role of the asparagine residue (Asn-353 in APA) by using site-directed mutagenesis to replace Asn-353 with a glutamine residue to keep the polarity, an alanine residue to abolish the polarity and an aspartate residue to introduce a negative charge. We first used immunofluorescence labeling of stable transfected CHO cells to ensure that the mutations did not modify the expression of mutated APAs at the plasma membrane (Figure 2A). The wild-type APA and the mutated APAs Gln-353 and Ala-353 exhibited similar membrane expression. In contrast, the Asp-353 mutant accumulated intracellularly and was not expressed at the plasma membrane (Figure 2A). Metabolic labeling and pulse-chase experiments of wild-type APA revealed an immunoprecipitated band with an apparent molecular mass of 140 kDa after 30 min of pulse and a second band of 168 kDa after 1 h of chase. Metabolic labeling and pulse-chase experiments of the mutated APAs revealed that the profiles of maturation for Gln-353 and Ala-353 mutated APAs were similar to that of the wild-type APA. In contrast, the Asp-353 mutant did not display the 168 kDa form of APA after 2 h of chase (Figure 2B). Wild-type and mutated APAs (Gln-353 and Ala-353) were purified by a single step purification assay as previously described by Iturrioz et al. (26). SDS-PAGE analysis revealed that wild-type, Gln-353, and Ala-353 APAs are similarly purified and that posttranscriptional modifications are not affected by either of these substitutions (Figure 3A). Western blotting with anti-Xpress antibody confirmed that the purified proteins were indeed recombinant His-APAs (Figure 3B). Purification of the Asp-353 mutant yielded a lower amount of the recombinant protein than that obtained with the other purifications and the recombinant protein exhibited a weak and unstable activity (data not shown).

Enzymatic Activity of Purified Recombinant His-APAs. The enzymatic activities of purified recombinant His-APAs were analyzed by determining the catalytic constants (K_m and k_{cat}) in standard conditions (presence of 4 mM Ca^{2+}) using GluNA, AspNA, and angiotensin II as substrates. The results are summarized in Table 1.

When the synthetic substrate GluNA was used, all the mutations led to a significant decrease in substrate hydrolysis as compared to the wild-type. Kinetic studies showed that this decrease was essentially due to an increase in K_m (11-fold for Gln-353 and 8-fold for Ala-353) and to a lesser extent to a decrease in k_{cat} (2-fold for each mutant) leading to a 24- and 14-fold decrease in the k_{cat}/K_m ratio for Gln-353 and Ala-353, respectively.

The replacement of Asn-353 with glutamine or alanine led to a significant decrease in AspNA hydrolysis as

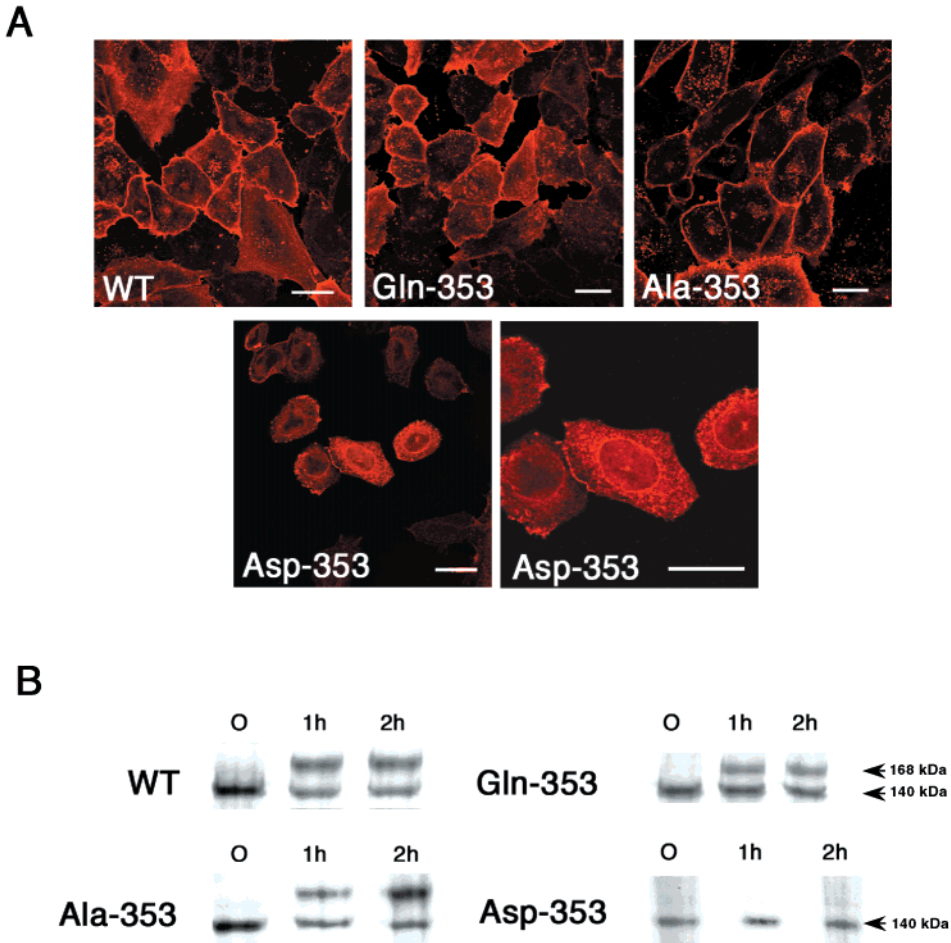


FIGURE 2: Expression and maturation of histidine-tagged wild-type and mutated mouse recombinant APAs. (A) CHO cells stably expressing the wild-type (WT) and mutated APAs (Gln-, Ala-, and Asp-353) were fixed and immunolabeled with a polyclonal rabbit anti-(rat APA) serum and revealed by use of an anti-mouse cyanin 3 conjugated antibody. Immunofluorescence was visualized by confocal microscopy. Bar = 20 μm . (B) CHO cells stably expressing WT and mutated APAs were labeled for 30 min with [^{35}S]methionine/cysteine and subjected to chase periods with serum free medium for various lengths of time. Solubilized cell-lysate proteins were immunoprecipitated with an anti-rat APA polyclonal antiserum, resolved by 7.5% SDS-PAGE and identified by autoradiography.

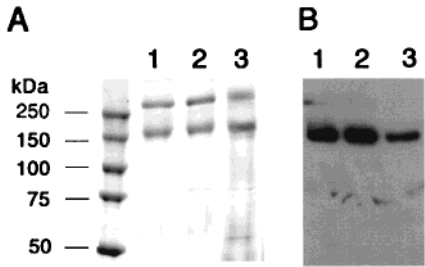


FIGURE 3: Purification of histidine-tagged mouse APA, wild-type, and mutants by Co^{2+} affinity chromatography. Pure CHO cell lines overproducing recombinant wild-type (WT) His-APA and mutated His-APA were established. Crude membranes were solubilized and subjected to metal affinity chromatography on a Talon column (Co^{2+}) as described previously by Iturrioz et al. (26). Material eluted from the Talon column [2.5 μg of protein in panel A and 0.125 μg of protein in panel B) was resolved by 7.5% SDS-PAGE and stained with Coomassie blue (A) or analyzed by Western blot using an anti-X-press antibody and resolved by ECL (B). Lines 1, 2, and 3 correspond to the cells transfected with the WT APA, Gln-353, and Ala-353 mutants, respectively. The high molecular weight band in the Coomassie blue stained gel corresponds to aggregated APA. The molecular mass markers used were 250, 150, 100, 75, and 50 kDa.

compared to the wild-type. The K_m values of the Gln-353 and Ala-353 mutants were 4 times higher than that of the wild-type, whereas the k_{cat} values were reduced by a factor

Table 1: Kinetic Parameters of Wild-Type and Mutated APAs ^a				
substrate	enzyme	K_m (μM)	k_{cat} (s^{-1})	k_{cat}/K_m ($\mu\text{M}^{-1}\text{s}^{-1}$)
Glu-NA	WT	243 \pm 26	404 \pm 33	1.663
	Gln-353	2687 \pm 779	184 \pm 75	0.068
	Ala-353	1943 \pm 140	227 \pm 9	0.116
Asp-NA	WT	515 \pm 52	102 \pm 5	0.200
	Gln-353	2272 \pm 220	25 \pm 2	0.011
	Ala-353	2307 \pm 14	14 \pm 1	0.006
Ang II	WT	73 \pm 4	20.0 \pm 2.0	0.271
	Gln-353	161 \pm 31	2.4 \pm 0.4	0.014
	Ala-353	62 \pm 20	4.8 \pm 0.9	0.077

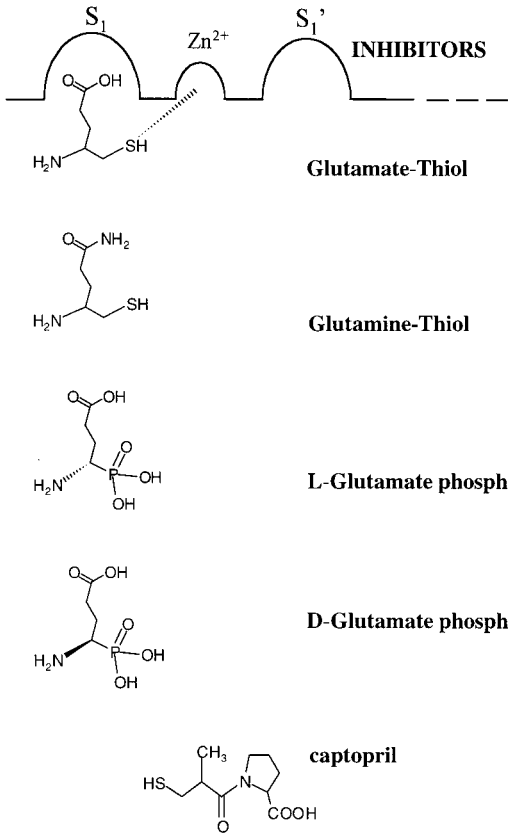
^a K_m and k_{cat} values are the means \pm the standard error of the mean of at least three separate experiments with duplicate determinations.

of 4 and 7, respectively. This resulted in a 18- and 33-fold decrease in the k_{cat}/K_m ratio of Gln-353 and Ala-353, respectively compared to that of the wild-type.

When the natural substrate angiotensin II was used, the K_m values of Gln-353 and Ala-353 were not significantly affected, whereas the k_{cat} values were reduced by a factor of 8 and 4, respectively. This resulted in a 19- and 4-fold decrease in the k_{cat}/K_m ratio of Gln-353 and Ala-353, respectively, compared to that of wild-type.

As previously shown, APA activity is dependent on the presence of Ca^{2+} (40). The Gln-353 and Ala-353 mutants

Table 2: K_i Values (μM) of Several Inhibitors on Wild-Type and Mutated APAs Using GluNA as Substrate^a

	INHIBITORS		
	WT	Gln-353	Ala-353
Glutamate-Thiol	0.216 ± 0.024	1.370 ± 0.004***	2.000 ± 0.390**
Glutamine-Thiol	0.462 ± 0.006	2.02 ± 0.38*	1.99 ± 0.43*
L-Glutamate phosphonic acid	0.060 ± 0.002	0.214 ± 0.019**	0.395 ± 0.068**
D-Glutamate phosphonic acid	3.31 ± 0.20	4.89 ± 1.90 n.s.	11.20 ± 0.20***
captopril	28.9 ± 6.8	14.1 ± 2.9 n.s.	24.8 ± 3.4 n.s.

^a K_i values are the means ± the standard error of the mean of at least three different experiments with duplicate determinations. (*) $p < 0.05$, (**) $p < 0.01$, (***) $p < 0.001$, n.s., no significant when compared to the corresponding wild-type value.

were activated by Ca^{2+} similarly to the wild-type enzyme, suggesting that the mutation does not modify the sensitivity to Ca^{2+} (not shown).

Inhibitory Potencies of Various Classes of Compound on Purified Recombinant His-APAs. To characterize further the function of Asn-353 in substrate or inhibitor binding, we evaluated the inhibitory potencies of various classes of compounds that differ either in their zinc chelating group or in their structure. The inhibitory potencies of these compounds were measured on GluNA (0.5 mM) hydrolysis by the wild-type and mutated enzymes at a supramaximal Ca^{2+} concentration (4 mM). The results are summarized in Table 2. The inhibitory potency of the substrate analogue (D,L-) GluSH ($K_i = 0.216 \mu\text{M}$) was decreased 6-fold for Gln-353 and 9-fold for Ala-353 compared to the wild-type enzyme (Table 2). The L-GluPO₃H₂, a pseudoanalogue of the transition state, was shown to be a potent inhibitor of APA ($K_i = 0.06 \mu\text{M}$) by the interaction of one of its phosphoryl oxygen with the zinc ion and the phenolic hydroxyl of Tyr-471 (25). The inhibitory potency of this inhibitor toward the mutant enzymes, Gln-353 and Ala-353, was significantly decreased (3.6- and 6.6-fold, respectively) compared to the wild-type enzyme. In contrast, the inhibitory potency of D-GluPO₃H₂ ($K_i = 3.31 \mu\text{M}$), was not significantly decreased for Gln-353 and was significantly decreased (3.4-fold) for Ala-353. The inhibitory potency of (D,L-) GlnSH was significantly decreased (4-fold) for both substitutions. The last compound, captopril, is a potent inhibitor of angiotensin-converting enzyme (ACE) (39). Captopril was also shown

to inhibit LTA4 hydrolase (41) and APA (27), despite the absence of a free amino group in its structure. This compound is a weak inhibitor of APA ($K_i = 29 \mu\text{M}$), and similarly inhibited the mutated and wild-type enzymes (Table 2).

DISCUSSION

In absence of a crystal structure of APA, site-directed mutagenesis is an important tool for probing the organization of its active site. Comparison of the sequence of APA with those of several monozinc aminopeptidases revealed a conserved motif, GXMEN, located at a constant distance (32 residues) from the HEXXH consensus motif (Figure 1). Site-directed mutagenesis of the glutamate of the GXMEN motif in APA and APN showed that this residue is implicated in substrate binding during catalysis by interacting with the free N-terminal part of substrates (27, 30). Thus, this residue is involved in the exopeptidase specificity of APA and of other monozinc aminopeptidases (27, 30). In contrast, the exopeptidase specificity of zinc metallopeptidases such as CPA is ensured by a basic residue (Arg-145 in CPA) and also by an asparagine residue (Asn-144 in CPA), which both bind the free-carboxylate group of substrates or inhibitors (31). The glutamate residue of the GXMEN motif was proposed to be the equivalent residue of Arg-145 in CPA. Moreover, the presence of an asparagine flanking the Glu-352 suggests that this residue plays a similar role to that of Asn-144 in CPA. To characterize further the GXMEN motif, we have investigated the function of Asn-353 in APA by replacing this residue with a glutamine, an alanine, or an aspartate by

site-directed mutagenesis. Confocal microscopy analysis allowed us to visualize APA expression at the plasma membrane of stable CHO cells expressing wild-type, Gln-353, and Ala-353 APAs and showed that these mutants are similarly routed to the wild-type APA. In contrast, the substitution of Asn-353 for an aspartate residue produced a recombinant protein that is not routed to the plasma membrane but remains trapped inside the cell, in perinuclear cisterna and in the large cytoplasmic network, which could correspond to endoplasmic reticulum (ER) (42). Metabolic labeling of stable transfected CHO cells expressing the wild-type APA followed by immunoprecipitation revealed the presence of two bands with a molecular mass of approximately 140 and 168 kDa corresponding to the low and high glycosylated forms of APA, respectively. The 140 kDa form corresponds to the high-mannose form of APA sorting from the ER, whereas the 168 kDa form corresponds to the mature complex glycosylated form sorting from the Golgi network (43). Moreover, Western blot analysis of the recombinant enzymes purified from a crude membrane preparation showed that the wild-type APA and the conservative mutants with neutral residues, Gln-353 and Ala-353, are similarly glycosylated (APA mature form of 168 kDa), suggesting that the replacement of Asn-353 with a glutamine or an alanine residue does not affect the biosynthesis, folding, or stability of the resulting proteins. In contrast, Asp-353, a mutant with an anionic charge substitution, only displayed the low glycosylated form and led to an inactive and unstable protein (data not shown). These observations show that the substitution of Asn-353 with an aspartate (a non conservative residue) causes a general disruption of the protein structure that does not allow the protein to move past the ER. This suggests that Asn-353 plays a role in the folding of APA.

The mutations (Gln-353 and Ala-353) led to a significant decrease in the hydrolysis of the synthetic substrates, GluNA and AspNA, as well as the natural substrate, angiotensin II (Ang II).

Kinetic studies in which GluNA was used as a substrate showed that the K_m values of both mutants decreased by 8- and 11-fold, respectively, compared to that of the wild-type, indicating that Asn-353 is involved in substrate binding. The k_{cat} values were slightly lowered (2-fold) for both mutants, reducing the k_{cat}/K_m ratio by a factor of 24 and 14 for Gln-353 and Ala-353, respectively. This indicates that Asn-353 is also involved in catalytic activity. When AspNA was used as a substrate, the K_m values of the mutants Gln-353 and Ala-353 were decreased 4-fold compared to that of the wild-type enzyme, confirming that Asn-353 is involved in substrate binding. The k_{cat} values of Gln-353 and Ala-353 were decreased by a factor of 4 and 7, respectively, lowering the k_{cat}/K_m ratio for both substrates by a factor of 18 and 33. However, the decrease in affinity of the mutated enzymes for the substrate AspNA was weaker than that observed in the presence of GluNA, whereas the reverse situation was observed for the k_{cat} values. Nevertheless, this led to similar decreases in the cleavage efficiency of both substrates.

Finally, we used the natural substrate Ang II which interacts in the APA active site not only with the S1 subsite but also with the other subsites (S'1, S'2, ...). In these conditions, the K_m values of the Gln-353 and Ala-353 mutants were not significantly modified. In contrast, the k_{cat} values were decreased by a factor of 8 and 4, respectively,

lowering the cleavage efficiencies of Ang II by a factor 19 and 4.

Together these data suggest that, depending of the length of the P1 lateral side chain of the substrate (Glu or Asp) and the number of amino acids of the substrate able to interact with the different subsites of APA, Asn-353 plays an important role in substrate binding during Michaelis complex formation and/or in catalysis.

Moreover, as the effects of the mutations were observed with substrates displaying only the P1 residue, this suggests that the interaction between Asn-353 and the substrate occurs in the S1 subsite. This probably explains why the effects of its mutation were more pronounced with a substrate that only interacts with the S1 subsite and not with a substrate that interacts with several subsites (such as Ang II).

We further investigated the function of Asn-353 in substrate binding by evaluating the mode of binding of various classes of inhibitors on the wild-type and mutated APAs. All the inhibitors used interact with the S1 subsite but differ in the nature of their zinc-chelating group, their side chain, or the orientation of their α -amino group. (i) The two β -aminothiol inhibitors, glutamate thiol (GluSH) (36) and glutamine thiol (GlnSH) (35), chelate the zinc atom via their thiol group and interact with the anionic site via their free N-terminal part but have different lateral chains: a carboxylate for GluSH and an amide group for GlnSH. The absence of the carboxylate slightly reduces the interaction with the S1 subsite. (ii) The α -aminophosphonate inhibitor, GluPO₃H₂ (37, 38), is a pseudoanalogue of the transition state. It is a potent inhibitor of APA, interacting with the S1 subsite and the anionic site but also with the zinc ion and the phenolic hydroxyl of Tyr-471 via one of its phosphoryl oxygen (25). The L- or D- conformations of GluPO₃H₂ were used. These two inhibitors only differ by the position of their α -amino group which strongly reduce the inhibitory potency of the D-GluPO₃H₂ isomer.

When Asn-353 was replaced with Gln-353 or Ala-353, the affinity of L-GluPO₃H₂ was significantly lowered (3.6- and 6.6-fold). In contrast, only the Ala-353 mutation induced a significant reduction in the affinity of the D-isomer of GluPO₃H₂ (3.4-fold). These data suggest that Asn-353 interacts with these inhibitors. Comparisons of the inhibitory potencies of L-GluPO₃H₂ and D-GluPO₃H₂ on the wild-type APA, revealed a 55-fold difference between the two K_i values. In the case of the Gln-353 and Ala-353 mutants, this difference was only 25-fold, indicating that the mutations modify the binding of the free N-terminal part of the inhibitor with the anionic binding site of APA. This implies that the carbonyl of the amide function of Asn-353 interacts with the free amino group of the inhibitor.

However, if Asn-353 exclusively interacts with the free NH₂ group of the inhibitor, this might lead to the absence of an effect of the Ala-353 mutation on the K_i value of D-GluPO₃H₂, which should remain identical to that of the wild-type. However, the substitution of Asn-353 with an alanine significantly decreased the affinity of this compound (3.4-fold). This suggests that another interaction exists between Asn-353 and this inhibitor.

The other interaction may be related to the lateral chain of the inhibitor. To test this hypothesis, we evaluated the effect of the Asn-353 mutations on the inhibitory potencies of GluSH and GlnSH. The alanine substitution diminished

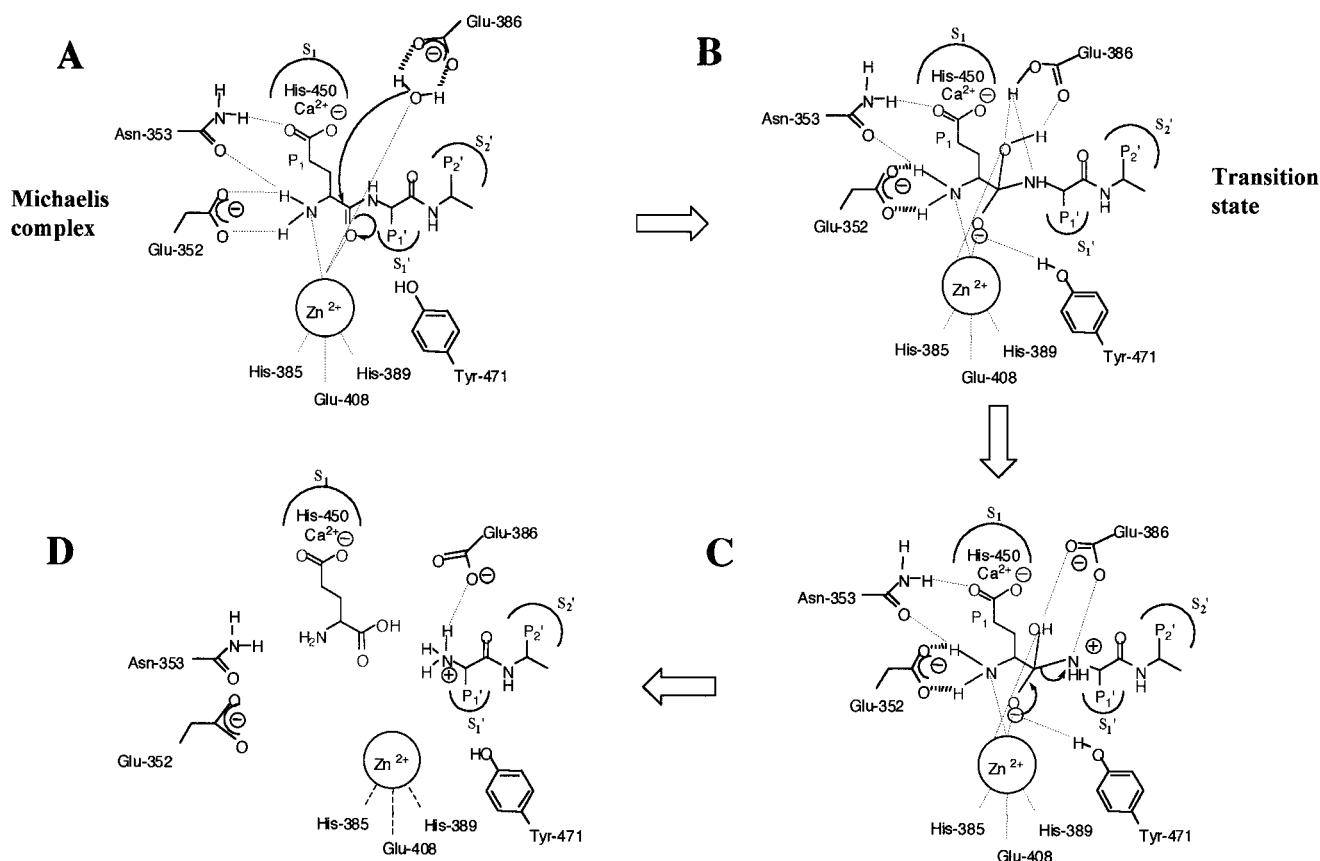


FIGURE 4: Putative catalytic mechanism of APA deduced from that of thermolysin proposed by Matthews (44) and taking previous site-directed mutagenesis studies on APA into account (24–27).

the affinity of GluSH by a factor of 9, but only decreased the affinity of GlnSH by a factor of 4, which is significantly different from that observed with GluSH.

This indicates that the NH_2 group of the amide function of Asn-353 may interact with the carboxylate side chain of the inhibitor. Finally, the K_i values of captopril were not modified by the mutations, suggesting that captopril does not interact with Asn-353. This correlates with the absence of the free amino group and an acidic side chain in this inhibitor.

The differential effect of the mutations on the kinetic parameters of GluNA and AspNA may be explained by this interaction between the NH_2 group of amide function of Asn-353 and the carboxylate side chain of these substrates. In fact, reducing the length of the glutamate side chain by one methylene group (Asp) may change the mode of binding of the substrate in the active site of APA.

A previous study on the GXMEN motif reported that Glu-352, which constitutes an anionic binding site of APA, interacts with the free N-terminal part of the substrate (27). Sequence comparison of several carboxypeptidases (Figure 1B) revealed two conserved asparagines and one conserved arginine in the NRN motif. Asn-144 and Arg-145 of CPA are thought to be responsible for the exopeptidase specificity of CPA, by interacting with the free C-terminal part of the substrates via hydrogen bonds (31). Our results suggest that Asn-353, located downstream of Glu-352, could be the functional equivalent of Asn-144. Interestingly, the exopeptidase specificity of APA and CPA is defined by two conserved motifs GXMEN and NRN, that would be structurally and functionally the mirror image of each other.

The recent resolution of the crystal structure of LTA4h in complex with the competitive inhibitor, bestatin, revealed that Glu-271 in the GXMEN motif interacts with the free N-terminal part of the inhibitor (28). This confirms our previous site-directed mutagenesis studies on APA showing that Glu-352 located in the GXMEN motif is responsible for the exopeptidase specificity of APA (27). A similar role was also proposed for Glu-350 in APN (30). The position of Glu-271 in the active site of LTA4h implies that Asn-272 of LTA4h (equivalent of Asn-353 in APA) is also positioned in the vicinity of the free α -amino group of the inhibitor. However, as bestatin is a weak inhibitor of LTA4h and is not an absolute analogue of the transition state, and as LTA4h is not strictly an aminopeptidase, the interaction between Asn-272 and bestatin was not mentioned by these authors. Conversely, the interaction between Asn-353 and the P1 carboxylate side chain of the substrate could be not observed in LTA4h due to the substrate specificity of this enzyme for N-terminal basic residues.

On the basis of this work and previous site-directed mutagenesis studies, we propose that GXMEN motif is responsible for the exopeptidase specificity of APA. Despite a very limited sequence similarity in APA, endopeptidases (TLN and NEP 24.11) and carboxypeptidases (CPA), the APA active site shares structural similarities with the active sites of these enzymes. This led us to propose a general catalytic mechanism of APA similar to that proposed for TLN deduced from X-ray diffraction studies (44). According to our model, in the absence of substrate, the zinc atom is tetracoordinated by three zinc ligands (His 385, His 389, Glu-408) and a water molecule. When the substrate enters in the

active site, its recognition and orientation are ensured by interactions with several residues. First, in the S1 subsite which only recognizes N-terminal acidic residues, Ca²⁺ and His-450 interact with the P1 carboxylate side chain of the substrate. In the anionic-binding site, Glu-352 and Asn-353 interact with the free N-terminal part of the substrate. In addition Asn-353 establishes a hydrogen bond with the P1 carboxylate side chain of the substrate. Simultaneously, the zinc atom becomes hexacoordinated by establishing two additional interactions with the carbonyl group of the scissile peptide bond and the unprotonated α -amino group of the substrate (Figure 4A). The negative charge of Glu-386 polarizes the zinc-coordinated water molecule and promotes its nucleophilic attack on the carbonyl carbon of the peptide bond to be cleaved. The resulting tetrahedral intermediate is stabilized by electrostatic interactions with the zinc ion and hydrogen bonds with Glu-386, Tyr-471, and Glu-352 (Figure 4B). Finally, the transfer of a proton from Glu-386 to the leaving nitrogen of the scissile peptide bond triggers the cleavage of the peptide bond and the release of products (Figure 4, panels C and D). In the absence of structural data on APA, our results contribute to the understanding of the organization of the active site of this enzyme. Moreover, by comparison with other metallopeptidases such as carboxypeptidases, endopeptidases, and double-zinc aminopeptidases, our work represents a basis for understanding the evolution of the zinc metallopeptidase family.

ACKNOWLEDGMENT

We thank Dr. S. Wilk and Dr. D. Healy for providing the APA antiserum, Dr. B. Lejczak for gift of the inhibitor GluPO₃H₂, and Prof. M.-C. Fournié-Zaluski for providing the inhibitors GluSH and GlnSH.

REFERENCES

- Nagatsu, I., Nagatsu, T., Yamamoto, T., Glenner, G. G., and Mehl, J. W. (1970) *Biochim. Biophys. Acta* 198, 255–270.
- Wilk, S., and Healy, D. (1993) *Adv. Neuroimmunol.* 3, 195–207.
- Lodja, Z., and Gossrau, R. (1980) *Histochemistry* 67, 267–290.
- Zini, S., Masdehors, P., Lenkei, Z., Fournie-Zaluski, M. C., Roques, B. P., Corvol, P., and Llorens-Cortes, C. (1997) *Neuroscience* 78, 1187–1193.
- Chauvel, E. N., Llorens-Cortès, C., Coric, P., Wilk, S., Roques, B., and Fournié-Zaluski, M. C. (1994) *J. Med. Chem.* 37, 2950–2956.
- Zini, S., Fournié-Zaluski, M. C., Chauvel, E., Roques, B. P., Corvol, P., and Llorens-Cortès, C. (1996) *Proc. Natl. Acad. Sci. U.S.A.* 93, 11968–11973.
- Reaux, A., Fournie-Zaluski, M. C., David, C., Zini, S., Roques, B. P., Corvol, P., and Llorens-Cortes, C. (1999) *Proc. Natl. Acad. Sci. U.S.A.* 96, 13415–13420.
- Reaux, A., Fournie-Zaluski, M. C., and Llorens-Cortes, C. (2001) *Trends Endocrinol. Metab.* 12, 157–162.
- Wu, Q., Lahti, J. M., Air, G. M., Burrows, P. D., and Cooper, M. D. (1990) *Proc. Natl. Acad. Sci. U.S.A.* 87, 993–997.
- Li, L., Wang, J., and Cooper, M. D. (1993) *Genomics* 17, 657–664.
- Nanus, D. M., Engelstein, D., Gastl, G. A., Gluck, L., Vidal, M. J., Morrison, M., Finstad, C. L., Bander, N. H., and Albino, A. P. (1993) *Proc. Natl. Acad. Sci. U.S.A.* 90, 7069–7073.
- Troyanovskaya, M., Jayaraman, G., Song, L., and Healy, D. P. (2000) *Am. J. Physiol. Regul. Integr. Comp. Physiol.* 278, R413–R424.
- Hesp, J. R., and Hooper, N. M. (1997) *Biochemistry* 36, 3000–3007.
- Jongeneel, C. V., Bouvier, J., and Bairoch, A. (1989) *FEBS Lett.* 242, 211–214.
- Hooper, N. M. (1994) *FEBS Lett.* 354, 1–6.
- Malfroy, B., Kado-Fong, H., Gros, C., Giros, B., Schwartz, J. C., and Hellmiss, R. (1989) *Biochem. Biophys. Res. Commun.* 161, 236–241.
- Watt, V. M., and Yip, C. C. (1989) *J. Biol. Chem.* 264, 5480–5487.
- Fukasawa, K. M., Fukasawa, K., Kanai, M., Fujii, S., and Harada, M. (1996) *J. Biol. Chem.* 271, 30731–30735.
- Cadel, S., Foulon, T., Viron, A., Balogh, A., Midol-Monnet, S., Noel, N., and Cohen, P. (1997) *Proc. Natl. Acad. Sci. U.S.A.* 94, 2963–2968.
- Schauder, B., Schomburg, L., Köhler, J., and Bauer, K. (1994) *Proc. Natl. Acad. Sci. U.S.A.* 91, 9534–9538.
- Funk, C. D., Radmark, O., Fu, J. Y., Matsumoto, T., Jornvall, H., Shimizu, T., and Samuelson, B. (1987) *Proc. Natl. Acad. Sci. U.S.A.* 84, 6677–6681.
- Rogi, T., Tsujimoto, M., Nakazato, H., Mizutani, S., and Tomoda, Y. (1996) *J. Biol. Chem.* 271, 56–61.
- Wang, J. Y., and Cooper, M. D. (1993) *Proc. Natl. Acad. Sci. U.S.A.* 90, 1222–1226.
- Vazeux, G., Wang, J., Corvol, P., and Llorens-Cortès, C. (1996) *J. Biol. Chem.* 271, 9069–9074.
- Vazeux, G., Iturrioz, X., Corvol, P., and Llorens-Cortes, C. (1997) *Biochem. J.* 327, 883–889.
- Iturrioz, X., Vazeux, G., Celerier, J., Corvol, P., and Llorens-Cortes, C. (2000) *Biochemistry* 39, 3061–3068.
- Vazeux, G., Iturrioz, X., Corvol, P., and Llorens-Cortes, C. (1998) *Biochem. J.* 334, 407–413.
- Thunnissen, M. M., Nordlund, P., and Haeggstrom, J. Z. (2001) *Nat. Struct. Biol.* 8, 131–135.
- Burley, S. K., David, P. R., Sweet, R. M., Taylor, A., and Lipscomb, W. N. (1992) *J. Mol. Biol.* 224, 113–140.
- Luciani, N., Marie-Claire, C., Ruffet, E., Beaumont, A., Roques, B. P., and Fournie-Zaluski, M. C. (1998) *Biochemistry* 37, 686–692.
- Christianson, D. W., and Lipscomb, W. N. (1989) *Acc. Chem. Res.* 22, 62–69.
- Herlitz, S., and Koenen, M. (1990) *Gene* 91, 143–147.
- Song, L., Ye, M., Troyanovskaya, M., Wilk, E., Wilk, S., and Healy, D. P. (1994) *Am. J. Physiol.* 267, F546–F557.
- Laemmli, U. K. (1970) *Nature* 227, 680–685.
- Chauvel, E. N., Coric, P., Llorens-Cortès, C., Wilk, S., Roques, B. P., and Fournié-Zaluski, M. C. (1994) *J. Med. Chem.* 37, 1339–1346.
- Wilk, S., and Thurston, L. S. (1990) *Neuropeptides* 16, 163–168.
- Lejczak, B., Kafaski, P., and Zygmunt, J. (1989) *Biochemistry* 28, 3249–3555.
- Lejczak, B., Choszczak, M. P. D., and Kafarski, P. (1993) *J. Enzyme Inhib.* 7, 97–103.
- Ondetti, M. A., Rubin, B., and Cushman, D. W. (1977) *Science* 196, 441–444.
- Glenner, G. G., McMillan, P. J., and Folk, J. E. (1962) *Nature* 194, 867.
- Orning, L., Krivi, G., Bild, G., Gierse, J., Ayken, S., and Fitzpatrick, F. A. (1991b) *J. Biol. Chem.* 266, 16507–16511.
- Louvard, D., Reggio, H., and Warren, G. (1982) *J. Cell Biol.* 92, 92–107.
- Stewart, J. R., and Kenny, A. J. (1984) *Biochem. J.* 224, 549–558.
- Matthews, B. W. (1988) *Acc. Chem. Res.* 21, 333–340.